

# In-Car GNSS Jammer Localization Using Vehicular Ad-Hoc Networks



**This article addresses the exciting notion of using vehicular ad-hoc networks to locate in-car jammers. Theoretical and experimental results confirm that localization based on this approach is indeed possible, with an error below 40 meters providing sufficient accuracy for determining the origin of an interference source. Limitations and future improvements of the test model are presented alongside its current successes.**

**DIANA FONTANELLA, ROLAND BAUERNFEIND,  
AND BERND EISSFELLER**  
UNIVERSITY FAF MUNICH

**G**NSS technology constitutes a fundamental element for new intelligent transport systems (ITSs) and their applications, such as advanced driver assistance, dangerous goods tracking, and distance-based toll systems. Due to the weak strength of navigation signals from distant satellites, however, these applications are threatened by malicious as well as unintentional interference.

In particular, so-called in-car jammers — also known as “personal privacy devices” — represent a serious threat for GNSS-based systems and applications. These jammers are cheap devices

able to obscure, partially or totally, the navigation signals received not only by the operator’s vehicle but also by other receivers in the vicinity.

The EC Standardization Mandate M/453 for cooperative ITSs provides a means to counter the interference threat. The introduction of standards for vehicular ad-hoc networks (VANETs) enables the exchange of data regarding detected interference events. This data exchange can be used to enhance the awareness of interference sources, allowing their localization and mitigation, thus increasing the reliability of future ITSs.

## **GNSS Interference Detection and Localization**

Interest in developing GNSS interference detection and localization capabilities

has increased steadily in the last few years. The first efforts in this direction have come for military applications, like the jammer detection and location (JLOC) system described in the news report, “Jammer Location Gets NGA Attention,” listed in the Additional Resources section near the end of this article). This system provides situational awareness on GPS interference events to U.S. military personnel and predicts effects worldwide to enhance battlefield situational awareness and mission planning.

In the case of identified GPS threats, the system disseminates alerts and reports to subscribed JLOC users through the SIPRNet (Secure Internet Protocol Router Network), a system of interconnected computer networks used

by the U.S. departments of defense and state to transmit classified information. The core element is the JLOC master station, operated by the U.S. National Geospatial-Intelligence Agency (NGA), which collects information on interference events through dedicated sensors incorporating GPS receivers. These sensors generate reports when they detect signal degradation as measured by carrier-to-noise ratio ( $C/N_0$ ) readings.

For the actual localization of the interference source, angle-of-arrival (AOA) information is collected from receivers capable of digital beam-forming, while time-difference-of-arrival (TDOA) measurements are computed with snapshots of data from multiple locations (further details in the article by A. Brown *et alia* in Additional Resources).

Further studies have been done to integrate mobile devices, such as cell phones, into the network of sensors. Also airborne sensors that can be carried on small unmanned aerial vehicles (UAVs) are envisaged for possible use in future jammer location systems.

Interference monitoring and localization systems have been developed to protect safety critical aviation services as required by the International Civil Aviation Organization (ICAO) for GPS-based approach procedures. In this application, location of interference sources is commonly based on direction-finding sensors. For example, in the United States the localization of interference is performed by the combined use of airborne (AIMDS), transportable (TIMDS), portable (PIMDS), handheld (HIMDS), and fixed (FIMDS) interference monitoring and detection systems. In Europe, similar systems are operated, such as the so-called GIMOS (GNSS Interference Monitoring System) in Germany.

The problem that can be caused for aviation by GPS jammers became very visible in November 2009 at the Newark Liberty International Airport (New York City). Without an appropriate interference localization system in place, it took more than three months to find the reason for periodic outages of the airport's

ground-based augmentation system (GBAS) reference stations: a GPS jammer transmitting from a vehicle passing near the airport. The airport eventually tackled the problem by making infrastructural changes, such as relocating the GBAS reference antennas over a wider area and enhancing interference detection and localization capabilities.

Based on recent flight inspection reports, civil aviation organizations need

held GPS interference detection devices. AOA, TDOA, and differential-received-signal-strength (DRSS)-based geolocation are currently under investigation.

Protecting all GNSS users, including the road transportation sector as well as users of portable navigation devices (PNDs), requires a much more comprehensive interference detection and localization system. Therefore, the U.S. Department of Homeland Security

### **Protecting all GNSS users, including the road transportation sector as well as users of portable navigation devices (PNDs), requires a much more comprehensive interference detection and localization system.**

to move beyond current direction-finding systems to high-resolution localization systems. The Additional Resources section lists articles about GIMOS and the November 2009 situation at Newark Liberty.

For maritime applications, the threat represented by jammers became evident in 2008, when the General Lighthouse Authorities of the United Kingdom and Ireland (GLA) conducted a series of sea-trials with the aim of characterizing the full effects of GPS jamming on safe navigation at sea (see the article by A. Grant *et alia*). The test unveiled serious effects on GLA differential GPS (DGPS) reference stations and GPS receivers on ships, as well as radar systems using GPS as their time reference.

These results gave rise to the GAARDIAN/SENTINEL projects. The GAARDIAN project developed and deployed probe sensors at various locations around the United Kingdom and Ireland to continuously report on the integrity, continuity, accuracy, and reliability of GPS signals. The monitoring network was then further expanded by including the Ordnance Survey's OS Net, consisting of more than 100 continuously operating GNSS receivers. This system bases detection of anomalies on a mask for  $C/N_0$  measurements.

The SENTINEL project later added interference localization capability to this network through the use of hand-

(DHS) is looking into deployment of a civil interference localization system, similar to the military JLOC system. The U.S. Interference Detection and Mitigation Plan (IDM), so-called "Patriot Watch", is currently under development as a national sensor capability (see the article by J. Merrill in Additional Resources).

The Patriot Watch architecture follows a system-of-systems approach with an open architecture where detected interference events shall be reported over a standardized interface. DHS has developed a central data repository for storage of all domestic GPS interference events. Initially, the plan links together existing government equipment including Federal Communications Commission (FCC) and Federal Aviation Administration (FAA) receiver sensors and UNITRAC.

UNITRAC is an information technology system that enables U.S. agencies to manage and monitor the location of GPS tracking terminals of designated resources. The U.S. IDM initiative envisions the integration of additional receiver networks such as the Continuously Operating Reference Stations (CORS) network of more than 1,800 GNSS stations operated by the U.S. National Geodetic Survey (NGS).

In the frame of the presented InCarITS project, an interference detection and localization network based on

GNSS receivers as part of a Cooperative Intelligent Transport System (C-ITS) infrastructure is proposed (see articles by R. Bauernfeind *et alia*). C-ITS applies information and communication technology to improve transportation efficiency, sustainability, and safety.

Primary technologies enabling C-ITS are:

- GNSS, by providing location information of vehicles
- vehicular ad-hoc networks (VANETs), which have been introduced in order to enable real-time communication of vehicle position and state
- floating car data (FCD), which enables the system to collect data on the vehicle environment with vehicle sensors
- local dynamic map (LDM), a geographical database managing the information.

Given the safety relevance of the interference threat to future C-ITS, detection and reporting of interference events should be included in the safety-related vehicular communication protocol and standardized accordingly.

## Vehicular Communication Standardization

In October 2009 the European Commission issued a mandate (M/453) inviting the European Standardization Organizations to prepare a coherent set of standards, specifications, and guidelines to support wide implementation and deployment of C-ITS within the European community. These focus on what are known as ITS stations (ITS-S), multi-technology packages that may be installed on vehicles or in roadside infrastructure.

Up to now, most of the standardization activities on ITS communication systems in Europe have been performed by the European Telecommunications Standards Institute (ETSI) Technical Committee on Intelligent Transport Systems in cooperation with the European Committee for Standardization (CEN). Harmonization between CEN and International Organization for Standardization (ISO) working groups

on cooperative Systems (CEN/TC278/WG16 and ISO/TC204/WG18) is also strongly supported.

The communication between nodes in a VANET face many unique challenges: factors such as high vehicle speeds, low signal latencies, varying topology, and scalability induce challenges that make conventional wireless technologies and protocols unsuitable for VANETs. The C-ITS communication link is based on the IEEE 802.11p standard with signals transmitted at 5.9 GHz (see Additional Resources).

The IEEE 802.11p standard describes the physical (PHY) layer and parts of the media access control (MAC) layer that will be adopted by ETSI within European Standard (EN) 202 663. In the ETSI context, this radio technology is called ITS-G5. Also ISO used IEEE 802.11p as possible access technology for its CALM standards. There the technology is called CALM-M5.

The ITS station positioning system is hosted at the application support facility layer. It permanently processes information received from the GNSS receiver and other vehicle sensors and combines them to obtain the ITS-S position information. The standardization of ITS-S position and time (ETSI/TC ITS/WG1) is a current work item (WI 0010013) and will be published within ETSI TS 102890-3.

The technical specification will provide information on position and time information used in messages and the data quality based on application requirements. Examples of safety applications under standardization are the Road Hazard Signalling (TS 101 539 - 1), the Intersection Collision Risk Warning (TS 101 539 - 2), and the Longitudinal Collision Risk Warning (TS 101 539 - 3). Currently defined position related parameters in the ITS cooperative awareness messages are: elevation, heading, latitude, longitude, horizontal position confidence as ellipse, and 95 % confidence level for longitude and latitude (see ETSI in Additional Resources). ITS standardization intends to allow flexible implementation of positioning technologies, but a common position

and time accuracy estimation method will be required.

The ongoing standardization process and the strong interest shown from the automotive industry in ITS applications suggest that this technology will be available in the near future. Because future C-ITS applications rely on the GNSS position, the system would definitely benefit from an interference detection and localization capability to protect the applications relying on it. Based on the communication architecture and the traffic management centers linked to local police forces, the ITS infrastructure could provide significant support for law enforcement with the capability to accurately locate the sources of interference.

## Jammer Localization: Theoretical Analysis

In this section we provide a mathematical description of the jammer localization problem. Vehicles surrounding a jamming device constitute an ad-hoc wireless sensor network (WSN) whose elements have an estimated knowledge of their own positions, provided by GNSS, possibly integrated with an inertial navigation system (INS) and map matching. In the following discussion the vehicles are referred to as sensors, elements, or nodes of the network.

**Measurements Model.** The localization system considered here includes elements with known coordinates and one element, the jamming source, which must be localized. Each sensor is identified by its own position vector known a priori,  $\vartheta_n = [x_n \ y_n]^T$ ,  $\{\vartheta_n\}_{n=1}^N \in \mathbb{R}^2$ , while the jammer position, indicated with  $\vartheta_j$ , is the unknown to be estimated. For simplicity of notation, we present the localization problem as though in a two-dimensional (2-D) space, however the extension to 3-D is straightforward.

The sensors are able to perform measurement functions of the distance between the sensor itself  $\vartheta_n$  and the interference source  $\vartheta_j$ ,  $d_n = \|\vartheta_n - \vartheta_j\|$ . Regardless of the measuring technique, a general model describing distance observations is given by:

$$m_n = h(d_n) + w_n \quad (1)$$

where both the distance function  $h(d_n)$  and the uncertainty  $w_n$  depend on the type of measurement and the surrounding environment.

In this case, we assume that the nodes perform power measurements defined as the in-band jamming power received by the GNSS receivers mounted on the vehicles. For received signal strength (RSS) observations, the log-normal path-loss model is commonly adopted (as described in the article by N. Patwari *et alia*). In this case,  $h(d_n)$  can be written as

$$h(d_n) = P_0 - P_n = P_0 - 10 \alpha \log_{10} \left( \frac{d_n}{d_0} \right) \quad (2)$$

where  $h(d_n)$  is the received power measured by sensor  $n$  in dBW, and  $P_0$  is the reference received power at distance  $d_0$ .  $\alpha$  is the path loss exponent of the propagation environment, which is considered to vary from two to five depending on the scenario.

Regarding the additive noise, fading is the most significant source of error for RSS techniques. When multiple signals with different amplitudes and phases arrive at the receiver, they add constructively or destructively as a function of the frequency, causing frequency-selective fading. In addition, shadowing causes environment-dependent errors. In outdoor environments, obstructions such as walls, trees, and buildings can attenuate the signal.

A common assumption is to consider the measurement uncertainties to be independent and unbiased, characterized by a standard deviation  $\sigma_w$ . In many cases, a Gaussian distribution can be motivated by the central limit theorem; so, for our purposes we assume  $w_n \sim N(0, \sigma_w^2)$ . Typical values for  $\sigma_w^2$  are within 4-12 decibels (see again N. Patwari *et alia*).

As stated before, because with passive localization we cannot retrieve the information on the power transmitted by the jammer, the system model proposed here makes use of DRSS measurements. This allows elimination of the unknown term  $P_0$  from the expression in (2).

For DRSS observations, the model becomes:

$$m_{n,\ell} = m_\ell - m_n = h(d_n, d_\ell) + \tilde{w}_{n,\ell} \quad (3)$$

where  $h(d_n, d_\ell)$  is defined as

$$h(d_n, d_\ell) = P_n - P_\ell = 10 \alpha \log_{10} \left( \frac{d_n}{d_\ell} \right) \quad (4)$$

and  $\tilde{w}_{n,\ell}$  is the sum of the two noise terms  $w_n$  and  $w_\ell$ .

Under the hypothesis of independent observations, the additive noise affecting DRSS measurements is Gaussian with zero mean and variance  $\sigma_{\tilde{w}}^2 = 2\sigma_w^2$ . In practical situations, this value will likely be lower because of spatially correlated noise contributions, as explained in the article by J. H. Lee and R. M. Buehrer (Additional Resources). Thus, we can write the noise variance as  $\sigma_{\tilde{w}}^2 = 2\sigma_w^2(1 - \rho_{n,\ell})$ , where  $\rho_{n,\ell} \in [0, 1]$  is the correlation coefficient reflecting the spatial correlation between the two sensor locations  $\vartheta_n$  and  $\vartheta_\ell$ . The worst case scenario (independent measurements) is represented by  $\rho_{n,\ell} = 0$ .

RSS methods are based on the path-loss propagation model. The estimated distance between the two network elements is directly proportional to the attenuation in signal power introduced by the channel propagation. The path-loss exponent,

which better represents the measurement environment, is in general an unknown parameter.

In order to retrieve the path-loss information, one possibility is to use predicted or measured spatial digital maps; another option is to jointly estimate  $\alpha$  as a nuisance parameter in the localization algorithm. The latter approach is expected to improve the estimation accuracy at the expense of requiring more measurements in order to estimate the jammer position. The problem of the path-loss exponent is further discussed with an experiment described later in this article.

**Maximum Likelihood Estimation.** Two classes of methods can solve the localization problem in a WSN: centralized methods, which collect measurements at a central unit prior to calculation, and distributed methods, which require sensors to share information only with their neighbors in an iterative fashion.

Considering the WSN jamming localization problem, VANETs are characterized by a highly dynamic scenario: the fast appearance and disappearance of nodes in the vicinity of an interference source makes the distributed localization quite difficult. For this reason it seems that the centralized approach is the most suitable one. Information related to the interference event can be transmitted by each node to the back-end office in charge of computing the jammer position as explained in the article by R. Bauernfeind *et alia* in Additional Resources.

In this study a centralized method based on maximum likelihood estimation (MLE) was adopted. The MLE is the optimal estimator criterion, as its accuracy asymptotically approaches the Cramér-Rao Lower Bound (CRLB) for increasing signal-to-noise ratio.

The MLE can be formulated as

$$\hat{\vartheta}_j = \arg \max_{\vartheta_j} \{ \ln [p(\mathbf{m} | \vartheta_j)] \} \quad (5)$$

where  $\mathbf{m}$  is the vector of DRSS measurements whose elements  $\{m_k\}_{k=1}^K \in \mathbb{R}$  are defined by (3), and  $p(\mathbf{m} | \vartheta_j)$  is the joint likelihood function of the measurements with respect to the unknown source position.

The number of differential measurements  $K$  depends on the number of sensors  $N$  (discussed in the J. H. Lee and R. M. Buehrer article). Among the total  $N(N-1)/2$  DRSS measurements, only a subset of  $N-1$  *basic* measurements is significant for the position estimation, while the others are *redundant*, meaning that they bring no further information. Here we assume that  $K = N-1$ , and the indices  $(n, \ell) \in [1, \dots, N]$  are mapped into index  $k \in [1, \dots, K]$ .

Considering the observations model explained previously, the joint likelihood distribution is formulated here as

$$p(\mathbf{m} | \vartheta_j) = \prod_{k=1}^K p(m_k | \vartheta_j) = \frac{1}{(2\pi)^{K/2} \sqrt{|\mathbf{Q}|}} \exp \left\{ -\frac{1}{2} (\mathbf{r}^T \mathbf{Q}^{-1} \mathbf{r}) \right\} \quad (6)$$

where  $\mathbf{r}$  is the vector of residuals whose elements are defined as  $r_k = m_{n,\ell} - h(d_n, d_\ell)$ , and  $\mathbf{Q}$  is the  $K \times K$  covariance matrix which, for independent observations, is diagonal and equal to  $2\sigma_w^2 \mathbf{I}$ .

In the hypothesis of spatially correlated noise, the expression of the elements of  $\mathbf{Q}$  becomes

$$q_{k,j} = \begin{cases} 2\sigma_w^2(1 - \rho_{n,\ell}), & k = j \\ \sigma_w^2(\rho_{n,p} - \rho_{p,\ell} - \rho_{n,q} + \rho_{\ell,q}), & k \neq j \\ 0 & \text{otherwise} \end{cases} \quad (7)$$

with  $(n, \ell)$  being the couple of sensors associated with  $k$  and  $(p, q)$  being the sensors associated with  $j$ . The expression of  $q_{k,j}$  on the second line occurs only when there is a common sensor between the two couples  $(n, \ell)$  and  $(p, q)$ .

The likelihood function is written as:

$$\mathcal{L}(\mathbf{m}|\vartheta_j) = -\frac{1}{2} [K^2 \ln(2\pi) + \ln(|\mathbf{Q}|) + \mathbf{r}^T \mathbf{Q}^{-1} \mathbf{r}] \quad (8)$$

In general no closed-form solution to the optimization problem in (5) exists, and a numerical search method is needed. This approach presents two main difficulties. First, the convergence of the algorithm is strongly influenced by initializing values: if they are not close to the correct solution, the optimization search could well converge to a local maximum. Besides, when measurements deviate from the assumed model, the results are no longer guaranteed to be optimal.

Lee and Buehrer propose and analyze a different estimation criterion based on the least-square (LS) solution. The two aforementioned issues however are always present for nonlinear optimization problems.

**Lower Bound.** The CRLB is a lower bound on the covariance of any unbiased estimator. Such a lower bound provides a useful tool for researchers and system designers — not only for testing localization algorithms but also for obtaining some understanding of the positioning performance with respect to the design parameters.

Here we present the expression of the CRLB on the position accuracy obtained with DRSS measurements. For more details on the mathematical derivation see the articles by N. Patwari *et alia* and R. J. R. Thompson *et alia* in Additional Resources.

The CRLB is defined as the inverse of the Fisher Information Matrix (FIM):

$$\mathbf{F}(\vartheta) = E[\nabla^T[\mathcal{L}(\mathbf{m}|\vartheta)]\nabla[\mathcal{L}(\mathbf{m}|\vartheta)]] \quad (9)$$

which can also be written element by element as follows:

$$\mathbf{F}(\vartheta) = \begin{bmatrix} f_{1,1} & f_{1,2} \\ f_{2,1} & f_{2,2} \end{bmatrix} = \begin{bmatrix} E\left[\left(\frac{\partial \mathcal{L}(\mathbf{m}|\vartheta)}{\partial x}\right)^2\right] & E\left[\frac{\partial \mathcal{L}(\mathbf{m}|\vartheta)}{\partial x} \frac{\partial \mathcal{L}(\mathbf{m}|\vartheta)}{\partial y}\right] \\ E\left[\frac{\partial \mathcal{L}(\mathbf{m}|\vartheta)}{\partial y} \frac{\partial \mathcal{L}(\mathbf{m}|\vartheta)}{\partial x}\right] & E\left[\left(\frac{\partial \mathcal{L}(\mathbf{m}|\vartheta)}{\partial y}\right)^2\right] \end{bmatrix} \quad (10)$$

The expression of the derivatives is given by

$$\frac{\partial \mathcal{L}(\mathbf{m}|\vartheta)}{\partial x} = \frac{10}{\ln 10} \sum_k r_k \sum_j \bar{q}_{k,j} \left( \frac{\Delta x_p}{d_p^2} - \frac{\Delta x_q}{d_q^2} \right) \quad (11)$$

$$\frac{\partial \mathcal{L}(\mathbf{m}|\vartheta)}{\partial y} = \frac{10}{\ln 10} \sum_k r_k \sum_j \bar{q}_{k,j} \left( \frac{\Delta y_p}{d_p^2} - \frac{\Delta y_q}{d_q^2} \right) \quad (12)$$

where  $d_n$  is the distance between sensor  $n$  and the jamming source as defined previously,  $\Delta x_n$  and  $\Delta y_n$  are the components of  $d_n$ , respectively, along the x- and y-axis;  $r_k$  is the residual



FIGURE 1 ISTA (left) and GATE (right) measuring vans at the parking place at the GATE site in Berchtesgaden

as defined earlier, and  $\bar{q}_{k,j}$  is the  $(k, j)$  element of the inverse covariance matrix,  $\mathbf{Q}^{-1}$ . For independent observations it stands that  $\mathbf{Q}^{-1} = 1/2\sigma_w^2 \cdot \mathbf{I}$ .

The elements of the FIM are obtained by substituting (11) and (12) into (10) and applying the average function:

$$f_{1,1} = \left( \frac{10}{\ln 10} \right)^2 \sum_k \sum_h q_{k,h} \gamma_k \gamma_h \quad (13)$$

$$f_{2,2} = \left( \frac{10}{\ln 10} \right)^2 \sum_k \sum_h q_{k,h} \delta_k \delta_h \quad (14)$$

$$f_{1,2} = f_{2,1} = \left( \frac{10}{\ln 10} \right)^2 \sum_k \sum_h q_{k,h} \gamma_k \delta_h \quad (15)$$

with the coefficients  $\gamma_k$  and  $\delta_k$  defined as follows:

$$\gamma_k = \sum_j \bar{q}_{k,j} \left( \frac{\Delta x_p}{d_p^2} - \frac{\Delta x_q}{d_q^2} \right) \quad (16)$$

$$\delta_k = \sum_j \bar{q}_{k,j} \left( \frac{\Delta y_p}{d_p^2} - \frac{\Delta y_q}{d_q^2} \right) \quad (17)$$

The CRLB covariance matrix is finally obtained as the inverse of the FIM,  $\mathbf{C} = \mathbf{F}(\vartheta)^{-1}$ .

## Jammer Localization: Open Field Measurements

Open field measurements in Germany's Galileo test area GATE (Galileo Test- und Entwicklungsumgebung) were performed in order to make a first assessment on the feasibility of jammer localization through VANETs. GATE Berchtesgaden is one of the five German outdoor test and development environments for Galileo and GPS satellite navigation. It consists of eight virtual Galileo satellites (ground transmitters) located on top of several mountains around the test area. The GATE site is characterized by a well-suited topology in order to support different testing scenarios and conditions.

For this measurement campaign two measuring vans were used, one belonging to the University FAF Munich's Institute of Space Technology and Space Applications (ISTA) and one provided by the GATE operators. The two vehicles are shown in **Figure 1**.

Both vans were equipped with the following devices (see Manufacturers section at the end of this article):

- a PC running the ISTA PC-based Experimental Software



FIGURE 2 Jamming devices used for the open field measurements

Receiver (ipexSR), a real-time multi-frequency GNSS receiver realized completely in software (Visual C++/ assembler), capable of recording a GNSS raw intermediate frequency (IF) signal stream for post-processing.

- a front-end designed for receiving L1 GNSS signals connected via USB cable to the PC. The gain of the front-end is set to be constant for all measurements.
- an An antenna mounted on the roof of the vehicle.

The front-end and antenna parameters are summarized in **Table 1** and **Table 2**.

Note that, in order to localize the jamming source in a 2D space, a minimum of three DRSS measurements is needed. This means that the localization experiment requires at least  $N = 4$  vehicles to have  $N - 3$  basic differential measurements.

Due to limited resources, however, a different approach was followed during the GATE tests performed in Berchtesgaden: one van was used as a reference sensor, whereas the second van was moved to simulate the other network sensors. In other words, instead of having a set of independent RSS measurements taken simultaneously from  $N$  different vehicles, a total of  $N - 1$  DRSS measurements were taken sequentially.

The precise positions of the reference receiver antenna, the moving receiver antenna, and the jamming device were recorded with the additional equipment available on the GATE van (GATE position feedback receiver system). This equipment is used in the GATE test area

to steer the virtual Galileo navigation signals.

Regarding the jamming source, a total of seven in-car jammers were available at ISTA (see **Figure 2**). The jammers were operated one at a time and in open conditions, i.e.,

they were fixed on a tripod at the same height as the receiving antennas and fed by a car battery.

Two experiments were realized in two different locations. The first experiment (Scenario A) studied the range of jamming signals and estimated the path loss exponent in the GATE test area. The second experiment (Scenario B) recorded the DRSS measurements as input for the jammer localization estimation.

All measurements were taken in static conditions. The jammer and reference receiver positions were chosen at the beginning of each experiment and kept constant. Regarding the moving receiver, its position was changed during the experiments in order to simulate the VANET, but the measurements were taken in static conditions.

**Scenario A.** The first goal was to study the interference range of each jammer under analysis. Depending on the jammer power level measured by the GNSS receiver, three different regions can be identified (see **Figure 3**): the first one is in the proximity of the interference source, where the interference power is so strong that the receiver front-end saturates (near region); the second region is an intermediate distance at which the received power level is proportional to the distance from the interference source according to a certain path-loss propagation law (intermediate region); the third region is where the jamming signal is too weak to be measured (far region).

In order for the localization algorithm to work, the sensors or vehicles need to be in the intermediate region. The identification of these three regions

is thus essential in order to set up a proper scenario for the experiments.

The area surrounding the interference source can be further divided into an area where the GNSS receiver tolerates the interference level and still provides position information (*GNSS area*), and an area where the jamming power is too strong for the receiver to work properly (*non-GNSS area*). The point at which the receiver passes from GNSS area to non-GNSS area is expected to be somewhere in the intermediate region (see **Figure 3**). In conditions of strong interference, an INS device embedded in the vehicle plays a fundamental role for a reliable estimation of the vehicles' positions.

Note that the identification of these regions and areas as previously defined depends on the measured power levels, and thus it changes depending on the particular GNSS receiver and jammer

Bandwidth	10.24 MHz
Sample Rate	20.48 MHz
IF Frequency	5.00 MHz
Quantization	8 bit

TABLE 1. Front-end parameters

Frequency	1575.42 ± 2 MHz
Gain (Preamp)	26 dB ± 3 dB
Gain (Antenna)	-1.0 dBic $0 \leq \theta < 75^\circ$
	-2.5 dBic $75 \leq \theta < 80^\circ$
	-4.5 dBic $80 \leq \theta < 85^\circ$
	-7.5 dBic $\theta < 90^\circ$

TABLE 2. Antenna parameters

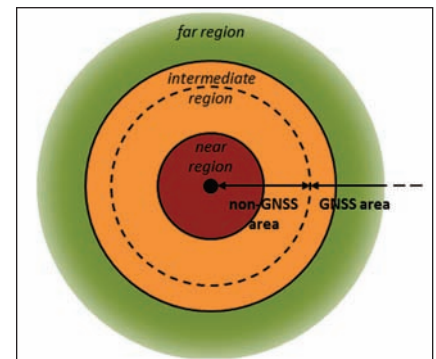


FIGURE 3 Scheme representing the different region and areas in the vicinity of an interference source

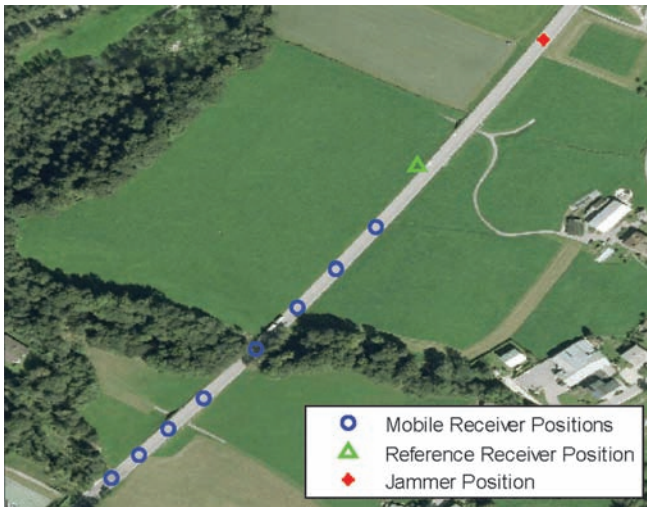


FIGURE 4 Scenario A: Positions chosen for jammer 3

considered. Table 3 gives a rough estimation of the intermediate region for each of the jammers under analysis. These distances were observed while driving the van along a straight street in the direction of the jammer and observing the quantization levels of the front-end in real time.

The second goal was to estimate the path loss exponent of the GATE test environment making use of the jamming signal. For this purpose, stationary measurements were taken while positioning the moving receiver at defined locations along the straight street, and keeping the reference receiver fixed in one location. Figure 4 shows the set up chosen for jammer 3.

IF sample streams of about 20 seconds were simultaneously recorded from the reference and moving receiver for each of the selected positions. The exact

location for each measurement point was provided by the GATE position feedback receiver system. The jammer was turned on about five seconds after the start of recording and the on/off transition was used to synchronize the measurements.

A sample pair of RSS measurements is displayed in Figure 5. The received

power is computed in post-processing from the recorded IF sample stream. We also normalized the power levels with respect to the noise floor. Finally, the two signals are synchronized on the on/off transition and cut on the same time support.

As can be observed from Figure 5, the power transmitted by the jamming device is not constant in time. For the localization strategy proposed here, the important information is represented by the difference between the two RSS streams, which is proportional to the ratio of inter-distances as described in the previously cited article by N. Patwari *et alia*.

Figure 6 shows the computed DRSS measurements with respect to the normalized distance from the interfering device (data set of jammer 3). The difference in received power is displayed (blue

asterisks) for each of the eight measurement positions shown in Figure 4, and the theoretical curves for two different values of path loss exponent are also shown.

Note that the first four mean values (red asterisks) fit to the curve with  $\alpha = 3$ , whereas the last four mean values fit to the curve with  $\alpha = 2.2$ . Looking at the layout of receivers and the jammer in Figure 4, a possible explanation for this effect is that the line of trees crossing the street are changing the propagation environment: when the moving van is on the same side as the jamming device (north), the trees generate reflections that degrade the received signal; when the moving van is beyond the trees (south), these create a sort of propagation tunnel so that only the line-of-sight (LOS) signal reaches the receiver.

The same experiment was repeated for all the jammers under analysis. The results obtained are all similar; so, they are not shown in order to save space in this article.

The conclusion of this study is that the GATE test area reflects the characteristics of a rural environment and a reasonable path-loss exponent to be considered for the localization estimation is between two and three. For a realistic application, the use of spatial digital maps seems to be a practical solution.

**Scenario B.** A different scenario was chosen for collecting the measurements to use in estimating the jammer location. In particular, a big crossroad

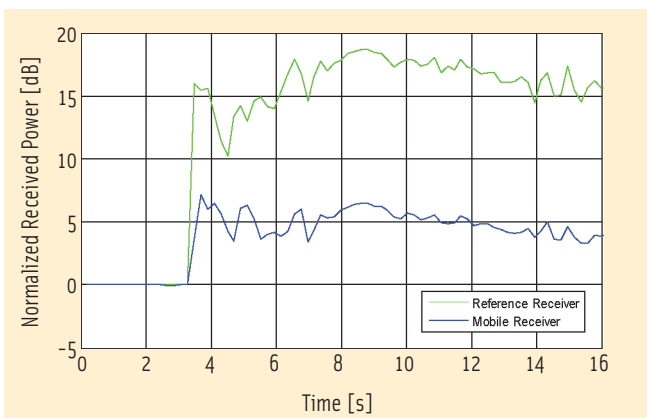


FIGURE 5 Scenario A: Pair of measurements taken from the data set of jammer 3

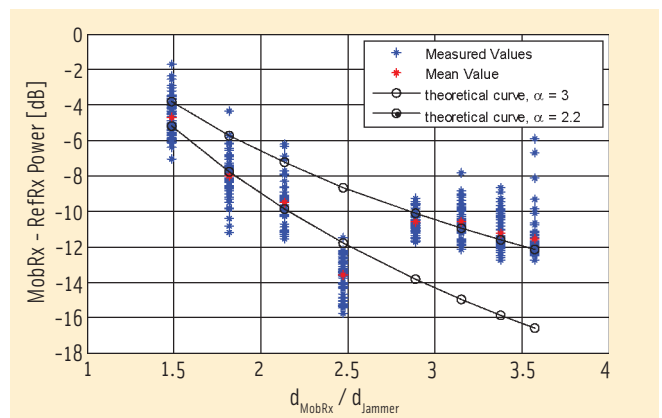


FIGURE 6 Scenario A: DRSS measurements for jammer 3

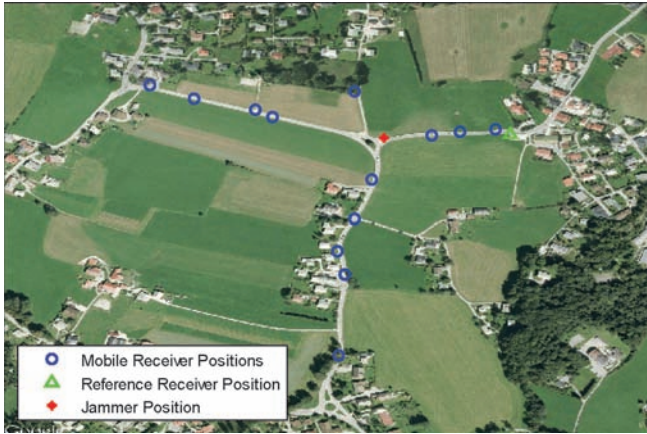


FIGURE 7 Scenario B: Positions chosen for jammers 2, 3, and 5 (group 1)

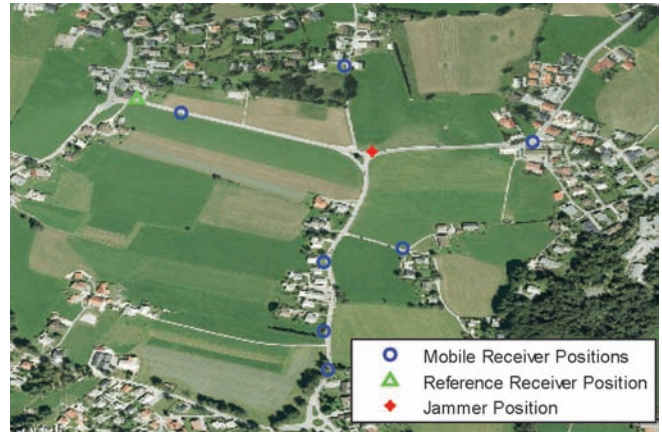


FIGURE 8 Scenario B: Positions chosen for jammers 6 and 7 (group 2)

seemed to be the best test environment for ensuring a small uncertainty region (see **Figure 7** and **Figure 8**).

As for the previous experiment, measurements were taken making use of two GNSS receivers mounted on two different vehicles, a moving and reference van. The reference receiver was located at a distance to the jammer where the front-end quantization of the received signal was optimal (no saturation). The moving receiver was placed at different sites during the recordings in order to simulate the presence of several vehicles (VANET).

Due to the different power levels emitted by the various interference devices, two sets of positions were chosen for jammers 2, 3, and 5 (group 1) and jammers 6 and 7 (group 2). Regarding jammers number 1 and 4, the first one transmits a low power and thus its intermediate region is too small to use for this experiment (see **Table 3**); the second one (number 4) was not working properly during the tests.

For the two previously mentioned groups of jammers under analysis, the following test procedure was followed:

- $T_0$ : The moving van is placed next to the reference receiver. Start of recording.
- $T_0 + 20$  seconds: The jammer is turned on.
- $T_0 + 40$  seconds: The moving van starts along the defined track, and stops at predefined stop points for about 20 seconds.
- $T_{end} - 40$  seconds: The moving van stops next to the reference receiver.

- $T_{end} - 20$  seconds: The jammer is turned off.
- $T_{end}$ : end of recording.

During this procedure the jammer was running continuously, with short interruptions at the endpoints of the route in order to allow for reacquisition of the GATE position feedback receiver, to enable a recalibration of the GATE system.

**Figure 9** shows an example of RSS measurements for jammer 3 computed in post-processing. The power levels are normalized with respect to the noise floor and the two signals are synchronized on the on/off transitions.

### Simulation Results

Starting from the IF sample streams recorded during the experiments, we computed DRSS measurements in post-processing for each of the measurement points. As already shown in Figures 7 and 8, 13 positions were chosen for group 1, and 7 positions were selected for group 2.

The DRSS measurements are used for localizing the jamming device through the ML estimation explained earlier. A path-loss exponent of  $\alpha$  equal to three and a noise variance  $\sigma_w^2$  of four decibels are considered. We assumed a covariance matrix  $\mathbf{Q}$  is diagonal since no

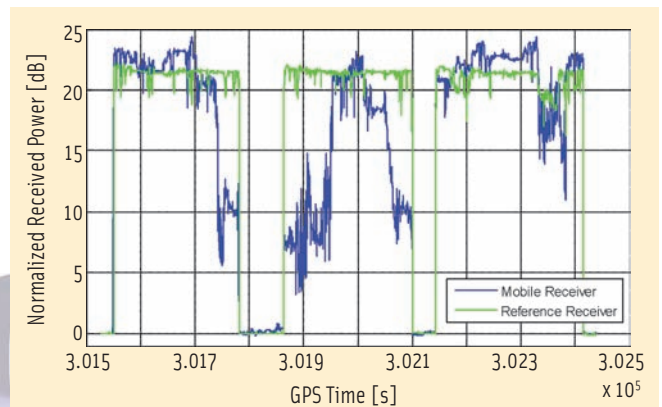


FIGURE 9 Scenario B: RRS measurements for jammer 3

Jammer #	Intermediate Region
1	(0,150 m)
2	(150 m, 2 km)
3	(<150 m,1.5 km)
4	N.A.
5	(0, 700 m)
6	(150 m, 2 km)
7	(200 m, > 3 km)

TABLE 3. Intermediate region for jammers under analysis

spatial correlation between sensors. Such an assumption is necessary in this case where the DRSS measurements were taken sequentially, and thus the fading affecting each of them is statistically independent.

For the nonlinear ML optimization, an iterative algorithm based on the method of trust region is adopted. Lee and Buerher describe this approach as the best one in terms of localization accuracy and robustness against a bad

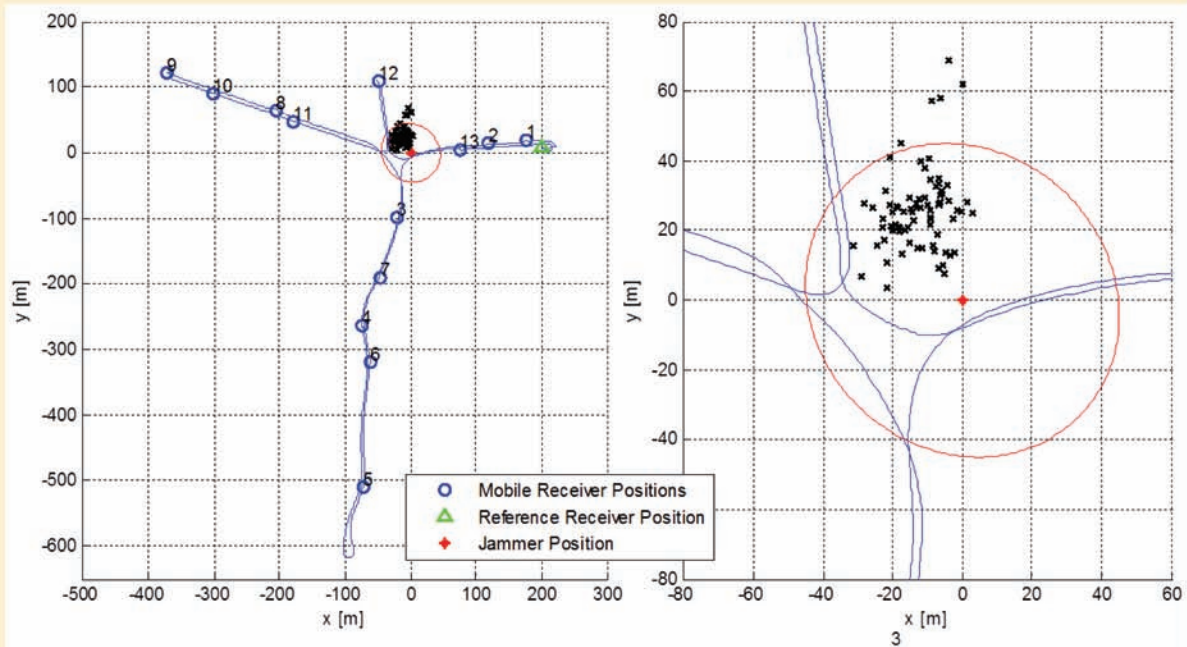


FIGURE 10 Jammer localization # 2

initial solution. Regarding the initialization, the first jammer position is extracted from a Gaussian distribution centered in the true coordinates with a standard deviation of 50 meters.

The position estimation for jammers number 2 and 7 are displayed in **Figure 10** and **Figure 11**. The estimated locations (100 samples) computed with the ML optimization are shown with black crosses; the 3- $\sigma$  uncertainty ellipse representing the CRLB is drawn in red. Only the results obtained for one jammer of each group here because of space considerations.

**Table 4** provides the CRLB on the estimation accuracy and the MLE variance and bias for all the jammers under study.

As expected, the position accuracy

obtained for jammers in group 1 is better than for group 2 as a result of the higher number of measurement positions.

Note that the ML estimation is quite accurate (small variance) but shows a substantial bias. The reason for this probably lies in the choice of the experimental set-up itself. That is, the bias likely depends on the reference receiver. In particular, all the DRSS measurements are obtained using a reference measurement recorded in the same position, which is not necessarily the case when a real VANET is deployed.

With the path-loss exponent the same for all the measurements, an over- or underestimation of it along the track from the jammer to the reference receiver generates an over- or underestimation of the inter-distance, which affects all the DRSS measures in the same way and gives rise to a bias. As a consequence, in this case the CRLB does not represent the lower bound on the estimation accuracy because the estimator is biased. It is

reasonable to assume that a different experimental set up making use of several measuring vans would allow for unbiased position estimation.

### Conclusion

In this article we have extensively discussed the potential for using VANETs to locate in-car jammers. Both from a theoretical and an experimental point of view, the results show that such a jammer-localization application based on VANETs is possible. As achieved in the CRLB estimation results, an error below 40 meters would probably be enough for public authorities to find the origin of an interference source.

Indeed the study case represents a specific scenario where the vehicles are placed all around the jammer (crossroad). This is in general not the case, especially along highways where the sensors are placed only along one direction. Map matching can be used for a good initialization of the localization algorithm and to set constraints in the estimation.

An additional note: use of two measuring vans recording sequentially from different positions instead of a set of vehicles operating at the same time

Jammer #	CRLB		MLE accuracy		
	$\sigma_x$ [m]	$\sigma_y$ [m]	$\sigma_x$ [m]	$\sigma_y$ [m]	bias [m]
2	8.5	8.5	5.7	7.9	31.2
3	8.5	8.5	4.2	1.6	48.6
5	8.5	8.5	8.4	9.2	168.7
6	31.6	31.5	68.7	18	107.9
7	31.6	31.5	34.5	13.1	86.9

TABLE 4. CRLB and ML estimation accuracy

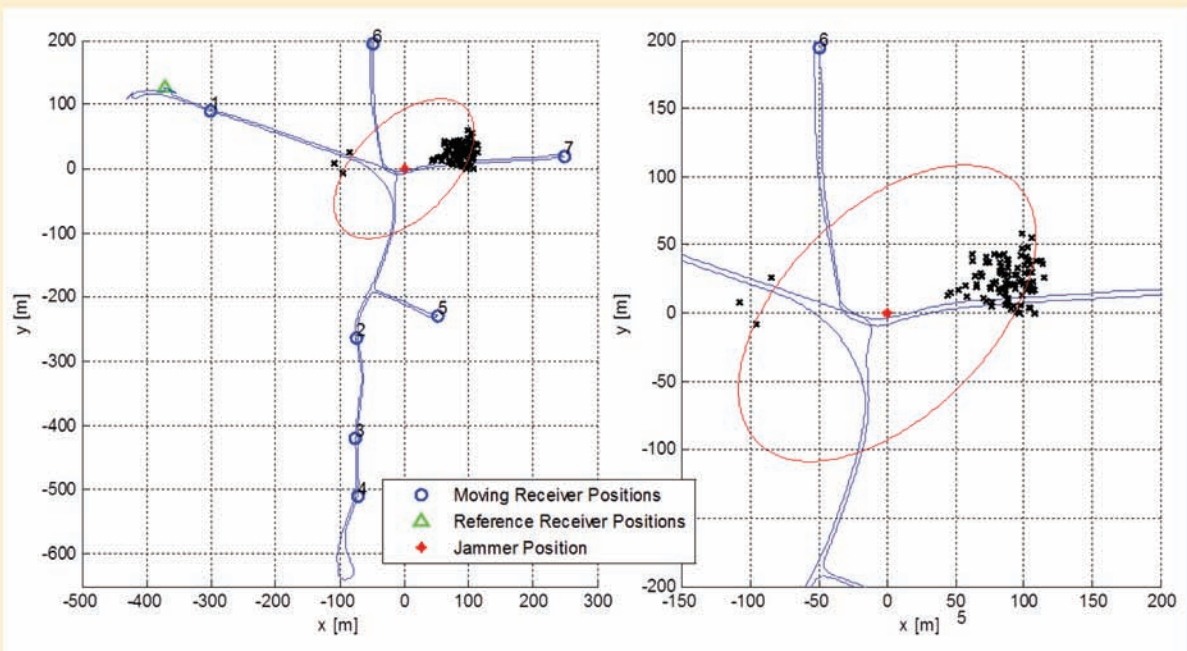


FIGURE 11 Jammer localization # 2

prevented the possibility of studying the effect of spatial correlation.

In the context of the current InCarITS II project, the localization algorithms are being further developed. The use of C-ITS infrastructure for cooperative interference and multipath mitigation techniques as well as cooperative relative positioning based on GNSS data exchange among vehicles is also being investigated.

For cooperative interference and multipath mitigation purposes, a local dynamic map can be used to develop situation awareness of the GNSS signal environment. As already mentioned, the LDM is a geographical database managing all relevant information related to the C-ITS infrastructure such as interference sources (e.g. DME transmitters). For cooperative multipath mitigation, the LDM can be used to provide a statistical description of the multipath environment based on the GNSS constellation and the current user-vehicle position. Finally, to enhance the accuracy of relative positioning in VANETs, techniques based on raw data exchange among vehicles can be used to mitigate common error sources and to obtain more accurate position solution.

## Manufacturers

**IfEN GmbH**, Poing, Germany, developed and operates the GATE Berchtesgaden facility. The RTK III is a front-end for receiving GNSS signals in the L1 frequency band, specifically developed by the **Fraunhofer Institute** for the ipexSR. A Model 511 antenna from **NovAtel, Inc.**, Calgary, Alberta, Canada, was mounted on the roof of the vehicle. The GATE position feedback receiver system consists of a NovAtel SPANSE GPS L1/L2 receiver with integrated FSAS-EI-SN inertial measurement unit from **iMAR Navigation Solutions**, St. Ingbert, Germany. The JLOC system mentioned in the article is the NAVSYS Jammer Detection and Location system from **NAVSYS Corporation**, Colorado Springs, Colorado USA. NAVSYS also developed the GPS Defender Android Application to demonstrate the integration of cell phones into JLOC.

## Acknowledgments

The results presented in this paper were developed during the InCarITS (Analysis, Detection and Mitigation of In-Car GNSS Jammer Interference in Intelligent Transport Systems, Grant No. 50NA1001) and InCarITS II (Inter-

ference Localization and Cooperative GNSS Signal Processing Algorithms for Intelligent Transport Systems, Grant No. 50NA1219) projects, funded by the German Federal Ministry of Economics and Technology (BMW) and administered by the Project Management Agency for Aeronautics Research of the German Space Agency (DLR) in Bonn, Germany.

## Additional Resources

- [1] Bauernfeind, R., and I. Kramer, H. Beckmann, B. Eissfeller, and V. Vierroth, "In-Car Jammer Interference Detection in Automotive GNSS receivers and localization by means of vehicular communication," *IEEE Forum on Integrated and Sustainable Transportation System (FISTS)*, 2011, vol., no., pp.376-381, June 29, 2011-July 1, 2011
- [2] Bauernfeind, R. and T. Kraus, A. Sicramaz Ayaz, D. Dötterböck and B. Eissfeller, "Analysis, Detection and Mitigation of In-car GNSS Jammer Interference in Intelligent Transport Systems," Deutscher Luft- und Raumfahrtkongress, Berlin, Germany, 2012
- [3] Brown, A., and D. Reynolds, and D. Roberts, "Jammer and Interference Location System - Design and Initial Test Results," ION GNSS 1999, Nashville, Tennessee USA, 1999
- [4] Butsch, F., *Untersuchungen zur elektromagnetischen Interferenz bei GPS*, Stuttgart: Universität Stuttgart, 2001

[5] Butsch, F., and O. Weber and W. Dunkel, "GNSS Interference Monitoring System GIMOS," 12th International Flight Inspection Symposium, Rome, Italy, 2002

[6] CEN, "CWA 16390 - Interface control document for provision of EGNOS CS/EDAS based services for tracking and tracing of the transport of goods," 2012.

[7] Dunkel, W. and F. Butsch, "GNSS Monitoring and Information Systems at Frankfurt Airport," *ION GNSS*, Salt Lake City, UT, 2000

[8] Directive 2004/52/EC of the European Parliament and Council (on the interoperability of electronic road toll systems in the Community), <<http://eurlex.europa.eu/LexUriServ/LexUriServ.do?uri=OJ:L:2004:166:0124:0143:EN:PDF>>, April 29, 2004

[9] ETSI, *TS 102 637-2; Intelligent Transport Systems (ITS); Vehicular Communications; Basic Set of Applications; Part 2: Specification of Cooperative Awareness Basic Service*. France, 2010-04

[10] ETSI, *TR 102 638; Intelligent Transport Systems (ITS); Vehicular Communications; Basic Set of Applications; Definitions*, 2009-06

[11] European Union, "Standardization Mandate M/453 of the European Commission addressed to CEN, CENELEC and ETSI in the field of information and communication technologies to support the interoperability of co-operative systems for intelligent transport in the European Community," October 2009, <[http://ec.europa.eu/enterprise/sectors/ict/files/standardisation\\_mandate\\_en.pdf](http://ec.europa.eu/enterprise/sectors/ict/files/standardisation_mandate_en.pdf)> (retrieved May 8, 2013)

[12] Evensen, K. and A. Csepinszky, *ITS Standardisation Handbook*, 2011: iCarSupport

[13] "GPS Jamming - No Jam Tomorrow," *The Economist*, March 2011

[14] Grabowski, J., "Personal Privacy Jammers: Locating Jersey PPDs Jamming GBAS Safety-of-Life Signals," *GPS World*, April 2012

[15] Grant, A., and P. Williams, N. Ward, and S. Basker, *GPS Jamming and the Impact on Maritime Navigation*, GLA, 2008

[16] ICAO, *DOC 8071 Manual on Testing of Radio Navigation Aids - Vol II Testing of Satellite-based Radio Navigation Systems Ed 5*, 2007

[17] *IEEE 802.11p-2010: Part 11: Wireless LAN Medium Access Control (MAC) and Physical Layer (PHY) Specifications: Amendment 6: Wireless Access in Vehicular Environments*, DOI: 10.1109/IEEESTD.2010.5514475, July 15, 2010

[18] "Jammer Location Gets NGA Attention," *GPS World*, pp. 12-14, July 2008

[19] Kraus, T., R. Bauernfeind, and B. Eissfeller, "Survey of In-Car Jammers - Analysis and Modeling of the RF Signals and IF Samples," *Proceedings*

of *ION GNSS 2011*, Portland, Oregon USA, September 2011

[20] Lee, J. H. and R. M. Buehrer, "Location Estimation Using Differential RSS with Spatially Correlated Shadowing," *Proceedings IEEE Global Communications Conference (GLOBECOM)*, 2009

[21] Merrill, J., "PatriotWatch, Vigilance Saving America," Workshop on Synchronization in Telecommunication Systems, 2012

[22] Patwari, N., and J. N. Ash, S. Kyperountas, A. O. Hero, R. L. Moses, and N. S. Correal, "Locating the Nodes: Cooperative Localization in Wireless Sensor Networks," *Signal Processing Magazine*, IEEE, Vol. 22, No. 4, pp. 54-69, July 2005

[23] Proctor, A. G., and C. W. Curry, J. Tong, M. Greaves, and P. Cruddance, "Protecting the UK Infrastructure: A System to Detect GNSS Jamming and Interference," *Inside GNSS*, September/October 2011

[24] Pullen, S. and G. Gao, G., "GNSS Jamming in the Name of Privacy," *Inside GNSS*, March/April 2012

[25] Pullen, S., and G. Gao, C. Tedeschi, and J. Warburton, "The Impact of Uninformed RF Interference on GBAS and Potential Mitigations," *ION International Technical Meeting 2012*, Newport Beach, California USA, 2012

[26] Rocchia, V., "Airborne RFI Detection: Examples of Solved Cases," 17th International Flight Inspection Symposium, Braunschweig, Germany, 2012

[27] Ströber, C., and M. Anghileri, A. Ayse Sicramaz, D. Dötterböck, I. Kramer, V. Kropp, J.-H. Won, B. Eissfeller, D. S. Güixens, and T. Pany, "ipexSR: A Real-Time Multi-Frequency Software GNSS Receiver," *ELMAR-2010 Proceedings*, September 2010

[28] Thompson, R. J., and A. T. Balaei, and A. G. Dempster, A. G., "Dilution of Precision for GNSS Interference Localization Systems," *Proceedings of ENC-GNSS*, 2009

**Authors**



**Diana Fontanella** received her M.Sc. in telecommunications engineering from Politecnico di Milano, Italy. Since 2010 she has been a research associate at the Institute

of Space Technology and Space Applications at the University of the Federal Armed Forces (UFAF) Munich. She is currently involved in European Space Agency (ESA) and French Space Agency (CNES) projects with a focus on GNSS signal design and performance assessment in dispersive

channel conditions. Her research interests include radio frequency compatibility and interference assessment as well as spoofing.



**Roland Bauernfeind** joined the Institute of Space Technology and Space Applications (formerly the Institute of Geodesy and Navigation) at the University of

Federal Armed Forces Munich in 2008 after a working at the German Space Operations Center as a satellite operations engineer. He received a diploma in aerospace engineering from University of Stuttgart. His main research topic is mitigation of man-made interference in GNSS receivers with focus on applications in intelligent transport systems.



**Bernd Eissfeller** is full professor of navigation and director of the Institute of Space Technology and Space Applications (formerly the Institute of Geodesy and Navigation) at the University FAF Munich. He is responsible for teaching and research in navigation and signal processing. Till the end of 1993 he worked in industry as a project manager on the development of GPS/INS navigation systems. He received the Habilitation (venia legendi) in navigation and physical geodesy and from 1994-2000 he was head of the GNSS Laboratory of the Institute of Geodesy and Navigation.



**Prof.-Dr. Günter Hein** serves as the editor of the Working Papers column. He is the head of the EGNOS and GNSS Evolution Program Department of the Euro-

pean Space Agency. Previously, he was a full professor and director of the Institute of Geodesy and Navigation at the Universität der Bundeswehr München. In 2002, he received the Johannes Kepler Award from the U.S. Institute of Navigation (ION) for "sustained and significant contributions" to satellite navigation. He is one of the inventors of the CBOC signal. 